Towards personalized and targeted treatment of head and neck cancer

Martens-de Kemp, S.R.

2014

Chapter 6

CD98 marks a subpopulation of head and neck squamous cell carcinoma cells with stem cell properties.

Stem Cell Res. 2013;10(3):477-88.

Sanne R. Martens-de Kemp
Arjen Brink
Marijke Stigter-van Walsum
J. Mirjam A. Damen
François Rustenburg
Thijs Wu
Wessel N. van Wieringen
Gerrit Jan Schuurhuis
Boudewijn J.M. Braakhuis
Monique Slijper
Ruud H. Brakenhoff

ABSTRACT

Patients with advanced head and neck squamous cell carcinomas (HNSCCs) are often treated with concomitant chemotherapy and radiotherapy, but only 50% is cured. A possible explanation for treatment failure is therapy resistance of the cancer stem cells (CSCs). The application of compounds specifically targeting these CSCs, in addition to routinely used therapeutics, would likely improve clinical outcome. We demonstrate that the previously described monoclonal antibody K984 recognizes the CD98 cell surface protein, which is specifically expressed by cells forming the squamous basal cell layer, the region where the squamous stem cells reside. Moreover, CD98 is highly resistant to the proteolytic enzymes required for CSC enrichment procedures. We show that $CD98^{high}$ cells, in contrast to $CD98^{low}$ cells, are able to generate tumors in immunodeficient mice, indicating that $CD98^{high}$ cells have stem cell characteristics. Furthermore, the $CD98^{high}$ subpopulation expresses high levels of cell cycle control and DNA repair genes, while the $CD98^{low}$ fraction shows expression patterns that represent the more differentiated cells forming the bulk of the tumor. CD98 is a promising CSC enrichment marker in HNSCC. Our data support the CSC concept in head and neck cancer and the potential relevance of these cells for treatment outcome.

INTRODUCTION

Cancer of the head and neck is the eighth most common cancer worldwide, with over 500,000 new cases diagnosed worldwide annually. Over 90% of the head and neck cancers are squamous cell carcinomas (HNSCCs). Despite advances in HNSCC diagnosis and treatment, mortality rates have remained high due to frequent development of locoregional recurrences and distant metastases. Patients with advanced stage HNSCC are most often treated with chemoradiation, *i.e.* the concurrent application of systemic cisplatin combined with locoregional radiotherapy. However, only 50-60% of the patients is cured[1,2] and there are currently no suitable parameters to predict a long-lasting curative response. Gene expression profiling on biopsies taken prior to chemoradiation did not result in gene sets with predictive significance[3].

It is generally hypothesized that not the bulk of cells in the tumor determines curative response, but only a small subpopulation, most likely the one that is referred to as the cancer stem cell (CSC) population. Recent studies have demonstrated that both haematological[4] and solid tumors[5] contain such a small subpopulation of cells. CSCs are able to self-renew and give rise to all differentiated cell lineages in a tumor. Several lines of evidence suggest that the CSC population is slow-cycling, possesses high levels of active detoxification pumps and DNA repair systems, and is therefore intrinsically resistant to anticancer treatments[6]. It was postulated that the CSCs originate from tissue stem cells that undergo a malignant transformation as a result of genetic changes[7-9]. Such a model has been proposed for squamous carcinogenesis as well[10]. The mucosal epithelium is formed by adjacent clonal units that consist of a single stem cell, multiple transit-amplifying cells and several layers of more differentiated cells. It is generally assumed that the stem cells reside in the basal cell layer. This tissue organization is retained in moderately and well differentiated squamous cell carcinomas. Mutations in the stem cells in the normal mucosal epithelium seem the initiating events in cancer development[10].

Over the past decade, CSCs from multiple solid tumor types have been isolated based on differential expression of protein markers on the cell membrane. CD44 is such a widely explored CSC enrichment marker. The CD44 protein is the cell surface receptor for hyaluronic acid[11] and mediates cell-cell and cell-matrix interactions. It was shown that the cancer stem cell concept is also relevant for HNSCC by demonstrating that CD44(+) cells are much more tumorigenic after serial transplantation in an immunodeficient mouse model than CD44(-) cells[12].

In the present study, we introduce a novel cell surface protein, CD98, that is specifically expressed on the cells of the basal layer and, in addition, remains stably expressed after a multitude of proteolytic treatments. We show that purified $CD98^{high}$ cells are able to induce tumor growth upon serial transplantation in mice. Moreover, $CD98^{high}$ cells show a significantly higher expression of genes involved in cell cycle control and DNA repair as compared to $CD98^{low}$ cells, whereas $CD98^{low}$ cells significantly express higher levels of genes involved in cellular differentiation, including keratinocyte differentiation. These findings support the CSC concept in HNSCC and suggest that CD98 can be exploited as a marker to enrich for CSCs in this tumor type.

MATERIAL AND METHODS

Cell lines, clinical specimens and animal models

The cancer cell lines used were all cultured in Dulbecco's modified Eagle's medium (DMEM), 5% fetal calf serum (FCS) and 2 mM L-glutamine, in a humidified atmosphere of 5% CO_2 at 37°C. Cell line VU-SCC-OE was derived from a moderately differentiated HNSCC tumor as described previously[13]. HNSCC cell lines UM-SCC-11B and UM-SCC-22A were obtained from Thomas Carey, PhD (University of Michigan, Ann Arbor, MI, USA)[14]. The Burkitt's lymphoma derived cell line Ramos was obtained from the American Type Culture Collection (USA), as was the pancreatic adenocarcinoma cell line BxPC3. Cell lines were authenticated by morphological

criteria, *TP53* mutation analysis and/or microsatellite markers.
The studies involving clinical specimens were approved by the Institutional Review Board, and only when patients consented to enrolment.
Female nu/nu mice were obtained from Harlan and the NOD/SCID IL2Rγ^{null} mice were ordered from Charles River. The significance of take rate differences was calculated using the Fisher exact probability test.

Characterization of the antigens recognized by MAbs K928 and K984
Antigens targeted by the K928 and K984 antibodies were identified by immunoprecipitation (IP) and mass spectrometry. Protein lysates were made from cell lines UM-SCC-22A (K984 identification), BxPC3 (K928 identification) and Ramos (negative control) and 500 µg of protein was used for IP. For IP, Dynabeads (Invitrogen) were employed according to the protocol of the manufacturer. The beads were coated with 4-6 µg K928 or K984 antibody. The P5D4 monoclonal antibody recognizing the HA hemagglutinin (HA) antigen was used as a negative control antibody. Electrophoresis of the isolated antigen was carried out on 7.5% (for K984) and 12.5% (for K928) SDS-polyacrylamide gels. Gels were fixed in 40% EtOH/10% acetic acid and stained with 2 mg/ml Coomassie blue R250 (Bio-Rad). Visible bands were excised and analyzed by mass spectrometry.

Mass spectrometry
Excised protein bands were reduced with DTT, alkylated with iodoacetamide and in-gel digested with trypsin[15]. Nanoflow liquid chromatography coupled to mass spectrometry was performed on an Agilent 1200 nanoflow system (Agilent technologies) connected to a FT(ICR)-MS (Thermo Fisher Scientific). The samples were trapped on a 20 mm Aqua C18 trapping column (Phenomenex; packed in-house, i.d., 100 µm; resin, 5 µm) with a flow-rate of 5 µL min^{-1}. Sequential elution of peptides was accomplished using an analytical column (Dr. Maisch GmbH, Germany; packed in-house, i.d., 50 µm; resin, 3 µm) with a 35 min gradient of 10–38% buffer B (buffer A, 0.1 M acetic acid; buffer B, 0.1 M acetic acid, 80% (v/v) acetonitrile) followed by 38–100% B in 3 min, 100% B for 2 min. The flow rate was passively split from 0.45 mL/min to 100 nL/min[16].
Nanospray was achieved using a distally coated fused silica emitter (New Objective) (o.d., 360 µm; i.d., 20 µm, tip i.d.10 µm) biased to 1.7 kV. The LTQ-FT(ICR) mass spectrometer was operated in the data dependent mode to automatically switch between MS and MS/MS. Survey full scan MS spectra were acquired from m/z 150 to m/z 1500 in the FT analyzer with a resolution of R=100,000 at m/z 400 after accumulation to a target value of 1,000,000 in the linear ion trap. The most intense ions at a threshold of above 500 were fragmented in the linear ion trap using collision-induced dissociation at a target value of 10,000.
Spectra were processed with Bioworks 3.1.1 (Thermo Fisher Scientific) and the subsequent data analysis was carried out using an in-house licensed Mascot search engine (version 2.1.02, Matrix Science). The FT(ICR) spectra were searched against the SwissProt Human database (version 56.2) with carbamidomethyl cysteine as a fixed modification. Protein N-acetylation, and oxidized methionines were set as variable modifications. Trypsin was specified as the proteolytic enzyme and up to one missed cleavage was allowed. The mass tolerance of the precursor ion was set to 30 ppm and that of fragment ions was set to 0.6 Da.

siRNA transfection
UM-SCC-11B cell cultures were transfected with siRNAs targeting *TROP2*, *CD98HC*, *CD98LC* or a combination of *CD98HC* and *CD98LC* mRNA. Cells were transfected with 25 nmol siRNA and 0.065 µl DharmaFECT1 (Dharmacon, Thermo Fisher Scientific). The nontargeting siCONTROL#2 and the *PLK1* SMARTpool were used as negative and positive control, respectively. Twenty-four hours post-transfection 60% of the transfection reagents was removed from the cultures and was

replaced with fresh growth medium. Another 72 hours later, cultures were visually inspected for cell death induced by *PLK1* knockdown. When the *PLK1* control confirmed efficient siRNA transfection, cells were either harvested using trypsin and stained with antibodies according to the FACS staining protocol or cells were lysed using ELB buffer (125mM NaCl, 50 mM Hepes pH 7.5, 0.1% NP-40 and 0.5 % Tween-20) for western blot analysis of gene knockdown.

Western blot analysis
Western blots were performed according to standard procedures. In short, gels were loaded with 40 µg protein. Anti-CD98 (1/400, clone H-300; Santa Cruz Biotechnology) detected the CD98 heavy chain and anti-β-actin (1/12,000, clone AC-15; Sigma-Aldrich) was used to control for equal loading. Proteins were visualized using commercially available secondary fluorescently-labeled antibodies (1/5,000 goat-anti-rabbit-IRDye 800CW and 1/5,000 goat-anti-mouse-IRDye 680 RD; LI-COR Biosciences).

Cell dissociation
UM-SCC-11B cells were seeded in T75 flasks (Greiner Bio-one) and grown until 70% confluency was reached. Cells were dissociated from the plastic bottom using one of the following reagents; 5 mM EDTA (Merck), trypsin-versene (EDTA) (Lonza), 1 mg/ml Collagenase IV (Sigma-Aldrich) or 500 µg/ml Liberase TH (Roche).

Tumor digestion
VU-SCC-OE cells were isolated from plastic culture flasks and inoculated subcutaneous in athymic nu/nu mice. Generated tumors (referred to as HNX-OE) were isolated from the mice in a sterile environment. Tumors were cut into small fragments, further minced using a sterile scalpel and incubated in a 500 µg/ml Liberase TH (Roche) solution in phosphate buffered saline (PBS) during 1 hour at 37°C. To stimulate the dissociation of the tumor cells, the mixture was resuspended every 15 minutes using a pipette. Resulting cell clumps were washed once with PBS/5% FCS and once with PBS. Cells were incubated subsequently in trypsin-versene (EDTA) (Lonza) during 15 minutes at 37°C. The enzyme was neutralized with PBS/5% FCS and the mixture was filtered through a 70 µm nylon mesh. Isolated cells were washed, counted and used for flow cytometry staining.

Flow cytometry
All steps in this process were performed at 4°C. Incubations were performed in 50 µl cold and sterile PBS/0.5% bovine serum albumin (BSA) per 10^6 cells. Fluorescently labeled antibodies were added in concentrations mentioned below and the samples were incubated during 30 minutes at 4°C in the dark. The K928 and K984 antibodies were DyLight 488 labeled using the DyLight microscale antibody labeling kit (Thermo Fisher Scientific). Anti-CD44 (V450-labelled, clone G44-26; BD Biosciences) was used in a 1:25 dilution, anti-CD98 (Fluorescein (FITC)-labeled, clone UM7F8; Santa Cruz Biotechnology) was used at a 1:20 dilution and anti-mouse H-2Kd (phycoerythrin (PE)-labeled, clone SF1-1.1; BD Biosciences) was diluted 1:200. Cells were washed three times with PBS/0.5% BSA and resuspended in 50 µl per 10^6 cells of PBS/0.5% BSA. To allow exclusion of non-viable cells, the stained cells were incubated with 7-Amino-Actinomycin D (7-AAD; BD Biosciences) during minimal 15 minutes at 4°C in the dark. Samples were resuspended in 300 µl per 10^6 cells of PBS/0.5% BSA. Sorting of cell populations was performed with a BD FACSAria flow cytometer (BD Biosciences). Subpopulations of cells were re-injected subcutaneously in NOD/SCID IL2Rγ^{null} mice (Charles River).

Immunohistochemistry
Frozen tissue sections were fixed during 10 minutes in 2% paraformaldehyde and pre-incubated for 30 minutes with 2% serum. Primary antibodies were incubated for 1 hour at room

temperature (anti-CD44, clone G44-26 (BD Biosciences); biotin conjugated anti-CD98, clone MEM-108 (Exbio); U36 (anti-CD44v6, own production); K928 (own production); K984 (own production)). A biotinylated anti-mouse antibody (Dako) was utilized as a secondary antibody combined with a horseradish peroxidase labeled strepavidin-biotin-complex (Vector Labs). Since the CD98 antibody was already biotin labeled, the application of a secondary antibody prior to the strepavidin-biotin-complex was not necessary. The staining was developed with diaminobenzidine and H_2O_2 as chromogen. Sections were counterstained with haematoxylin and cover slipped with Kaiser's glycerin.

Formalin-fixed paraffin-embedded sections of HNSCC tumors were deparaffinized and subjected to Tris/EDTA (pH 9.0) antigen retrieval. Primary antibodies, U36 (anti-CD44v6, own production) and anti-CD98 (clone H-300, Santa Cruz Biotechnology), were diluted in PBS containing 2% goat serum and incubated overnight at 4°C. Afterwards, the BrightVision +Poly-HRP-Anti Ms/Rb/Rt IgG kit (Immunologic BV,) was employed according to the description of the manufacturer. The staining was developed with diaminobenzidine and H_2O_2 as chromogen. Sections were counterstained with haematoxylin and cover slipped with Kaiser's glycerin.

Gene expression microarrays

Four HNX-OE tumors were separately prepared for flow cytometry analysis and sorting procedures as described above. For each tumor the $CD98^{high}$ and $CD98^{low}$ fractions were collected and the RNA was isolated. cDNA synthesis and labeling were performed according to the recommendations of the manufacturer (Agilent Technologies), including quality controls (QCs). One of the $CD98^{low}$ cell fractions did not pass QC and was not used for microarray analysis. Hybridization was performed on a human GE 4x44K formatted expression array spotted with 60-mer oligonucleotides representing over 43,000 well-characterized coding and non-coding sequences (G4112F, Agilent Technologies).

All analyses of the gene expression microarray data were done within the R statistical software, using the Limma-package. Preprocessing of the gene expression data comprised of RMA background correction, loess within-array normalization and A-quantile between-array normalization. Single channel data were used to accommodate the unbalanced design (four $CD98^{high}$ samples versus three $CD98^{low}$ samples). The moderated t-test implemented in Limma, employing empirical Bayes estimation of the variance, was used to evaluate the difference in gene expression between the two groups. Sample origin and CyDye were taken along as possible confounders. The Benjamini-Hochberg procedure was applied to the raw p-values to control the False Discovery Rate (FDR).

RESULTS

MAb K984 is specifically expressed on basal cells and targets the CD98 antigen

Previously, our group generated a panel of monoclonal antibodies to squamous cell carcinoma surface antigens[17]. It was shown that MAbs K984 and K928 have complementary staining patterns which relate to cellular differentiation in normal squamous epithelia. MAb K984 targets the undifferentiated cells of the basal layer in which the stem cells are assumed to reside, while MAb K928 is specifically expressed on the differentiated cells in the suprabasal layers (Fig. 1A). To determine the antigens recognized by these MAbs, we performed immunoprecipitation (IP) with the antibodies and analyzed the pulled down proteins with mass spectrometry. The K928 antibody was shown to recognize a calcium signal transducer encoded by *TACSTD2* (*TROP2*). Knockdown of *TACSTD2* expression by small interfering RNA (siRNA) in cultured UM-SCC-11B cells showed a decrease in K928 associated fluorescent signal as monitored by flow cytometry (Fig. 2A). Analysis of the IP product obtained with MAb K984 showed that this antibody recognizes the CD98 glycoprotein, which consists of a heterodimer of a heavy chain (CD98HC) and a light chain (CD98LC). Indeed, a commercially available CD98 antibody showed a staining

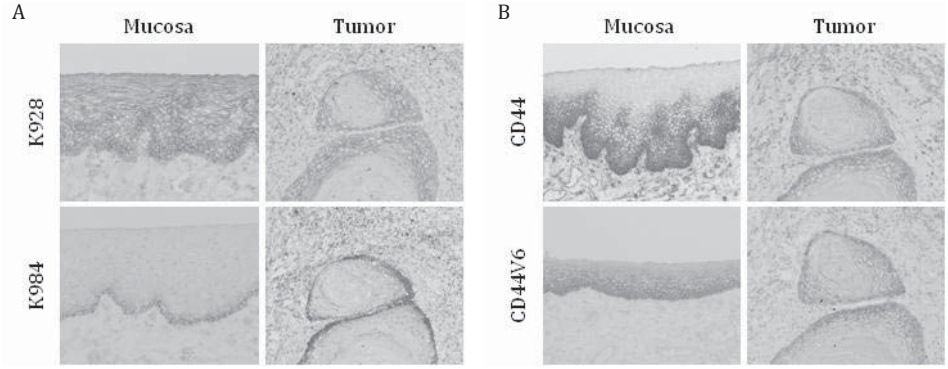

Figure 1. Immunostaining patterns of MAb K984, MAb K928 and anti-CD44.
(A) Immunohistochemical analysis of K928 and K984 staining patterns in fresh frozen normal mucosa and HNSCC. MAb K928 typically targets the differentiated suprabasal cells, whereas the antigen recognized by MAb K984 is expressed in the basal layer. Staining patterns observed with these antibodies are complementary. Pictures from mucosa samples were taken using a 20x magnification and the pictures from the tumor samples with a 10x magnification. (B) Immunohistochemical analysis of CD44 and CD44v6 expression in fresh frozen normal mucosa and HNSCC. Both basal and suprabasal cells show CD44 expression, but highest expression was visible in the basal cells. Pictures were taken with a 10x magnification.

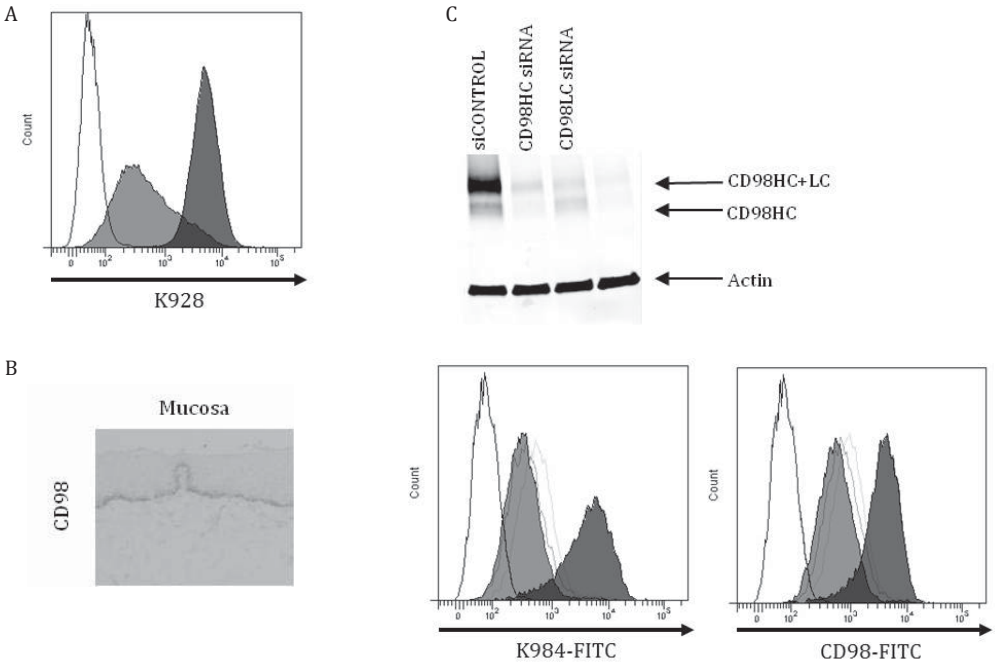

Figure 2. Characterization of the antigens recognized by MAbs K984 and K928.
(A) TACSTD2 siRNA transfected UM-SCC-11B cells were stained with a FITC-labeled K928 antibody. A non-targeting siCONTROL#2 siRNA was used as a positive control (black). Knockdown of *TACSTD2* resulted in a decrease in K928 fluorescent signal of 83% (grey). The negative control is represented in white. Similar results were seen in a different HNSCC cell line (data not shown). (B) Immunohistochemical CD98 staining using a commercially available antibody on normal mucosa (10x magnified) shows a staining pattern similar to that of K984 (see Fig. 1A). (C) UM-SCC-11B cells were transfected with siRNAs targeting either *CD98HC*, *CD98LC* or a combination of both. Western blot analysis confirmed the knockdown of CD98HC and implicated the inability to form the CD98HC+LC complex in the absence of CD98LC (upper panel). *CD98* siRNA transfected cells were analyzed for K984 and CD98 expression by flow cytometry (lower panel). White peaks indicate negative control measurements and the non-targeting siCONTROL siRNA was used as a positive control (black peaks). When compared to siCONTROL transfected cells, both the cell populations transfected with *CD98LC* or *CD98HC* (grey lines) siRNAs showed a reduced K984 fluorescent signal (at least 86% reduced), as does the combination of these siRNAs (grey peak). Control measurements with a CD98 antibody (right panel) showed the same pattern (at least 71% reduction in fluorescent signal). Similar results were obtained using a different HNSCC cell line.

pattern similar to K984 in normal mucosa (Fig. 1A and 2B). SiRNA mediated knockdown of *CD98* (either the heavy chain, the light chain or both) resulted in a decrease in both K984 and CD98 signal intensity in cultured UM-SCC-11B cells (Fig. 2C). Cellular morphology was not altered due to the knockdown of any of the siRNA target sequences (Supplementary Fig. S1).

CD98 positive cells also express stem cell marker CD44v6

Since squamous stem cells are assumed to reside in the basal cells, and as CD98 is specifically expressed by these basal cells, both in normal mucosa as well as moderately and well-differentiated tumors, we hypothesized that selection of CD98^{high} cells might allow enrichment of the squamous CSCs. First, we compared the expression of CD98 with that of the known CSC marker CD44 by immunohistochemistry. There are several CD44 isoforms present in both normal mucosa and malignant squamous tissues[18]. We therefore tested an antibody recognizing all CD44 isoforms and an antibody specifically recognizing the CD44v6 isoforms in the same tissue as used previously for CD98 (Fig. 1B). We noted that the staining patterns on squamous cells between these two antibodies appear very similar, but the staining pattern on stromal cells differs as expected. The basal cells in the mucosal epithelium express a higher level of CD44/CD44v6 than the suprabasal cells, supporting the hypothesis that the mucosal stem cells reside within these basal cell layers. Furthermore, we compared the CD98 immunohistochemical staining pattern to that of CD44v6 in several HNSCC tumor specimens (Fig. 3) and concluded that the CD98 expression overlaps considerably with that of CD44v6 in HNSCC tumors. These data support the hypothesis that CD98 might target CSCs, as was previously described for CD44.

CD98 antigen is resistant to proteolytic cleavage

One of the characteristics of CSCs is that they can be isolated on the basis of a cell surface marker with techniques like FACS sorting. As proteolytic enzymes are required to make single cell suspensions from human solid tumors or xenografts, we tested whether the CD98 antigen is stable under several proteolytic conditions. For comparison, we tested the stability of CD44 expression after incubation with the same proteolytic enzymes (Supplementary Fig. S2). We knew from FACS experiments (Fig. 2C) that CD98 is trypsin resistant and we investigated the stability of the CD98 antigen under several proteolytic conditions. UM-SCC-11B and VU-SCC-OE cells were grown in tissue culture and treated with a variety of proteolytic enzymes. Single

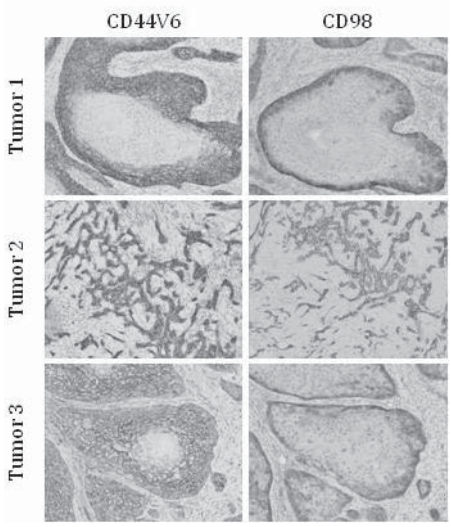

Figure 3. CD98 expression is restricted to a smaller cell population than CD44v6.
Several formalin-fixed paraffin-embedded (FFPE) HNSCC specimens were subjected to immunohistochemical staining procedures for CD44v6 and CD98. Pictures were taken using a 10x magnification.

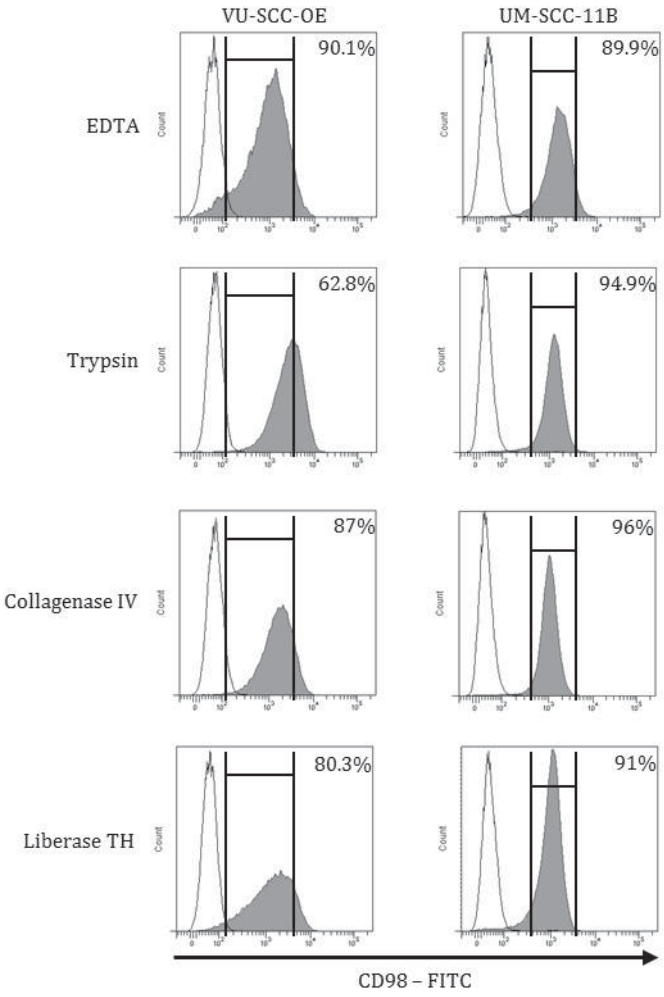

Figure 4. CD98 expression is resistant to proteolytic enzymes.
VU-SCC-OE (left) and UM-SCC-11B (right) cell cultures were harvested from plastic flasks using indicated proteolytic enzymes. EDTA was applied as a positive control. A commercially available FITC-labeled CD98 antibody was used to analyze CD98 expression by flow cytometry. White peaks represent negative control measurements and black peaks indicate CD98 expression. We gated 90% of the events in the EDTA control measurement. No decrease in CD98 expression could be determined with any of the enzymes as compared to the EDTA control ($p \geq 0.1$, two-tailed Fisher exact probability test). Figures are representative for at least duplicate experiments.

cell suspensions were subsequently incubated with a CD98 antibody and analyzed with flow cytometry (Fig. 4). A strong fluorescent signal was detected in the cell cultures treated with EDTA, which was used as a positive control. Also the cell populations harvested with the other enzyme-containing solutions (trypsin, collagenase IV and Liberase TH) did not show a decrease in fluorescent signal, as compared to EDTA treated cells. This indicates that the CD98 antigen is highly resistant to proteolytic cleavage and is therefore a stable marker that can be used for CSC isolation by FACS sorting. CD44 seems more sensitive to proteolytic degradation, but this depends on the enzyme used and the cell line tested (Supplementary Fig. S2).

The HNSCC stem cell population is enriched in CD98^{high} cells

All previous data support the idea that CD98 could be used for the enrichment of squamous CSCs. First, the proper mouse model for stem cell experiments was chosen based on an initial take rate experiment. A limiting dilution analysis was performed using VU-SCC-OE cells harvested from tissue culture in athymic nu/nu (nude) mice, our standard mouse model, and NOD/SCID mice lacking the interleukin-2 gamma receptor (NOD/SCID IL2Rγ^{null}). Take rates were considerably higher in NOD/SCID IL2Rγ^{null} mice than in nu/nu mice (Supplementary Table S1). Injection of only 25 cells initiated the growth of a tumor in 1 of 14 injection sites. Furthermore, palpable tumors were registered earlier in the NOD/SCID IL2Rγ^{null} mice and tumors in these mice grew faster than in the nu/nu mice (data not shown). Based on these results we used the NOD/SCID

Table 1. First serial transplantation of CD98^{high}, CD98^{low} and unselected HNX-OE cells in NOD/SCID IL2Rγ^{null} mice.

Population	No. tumors/no. injections			Days to first palpability
	Cells injected			
No of cells	25,000	2,500	250	
CD98^{high}	4/6	0/6	0/6	34±1
CD98^{low}	0/6	0/6	0/6	NA
Unselected	1/6	0/6	0/6	54

Abbreviation: NA, not applicable

IL2Rγ^{null} mice for further experiments.

HNX-OE donor tumors, derived from VU-SCC-OE cells injected in NOD/SCID IL2Rγ^{null} mice, were immunostained for CD98 and sorted into a CD98^{high}, a CD98^{low} and an unselected fraction. Cell dilutions of the different fractions were inoculated in NOD/SCID IL2Rγ^{null} mice and tumor growth was monitored (Table 1). Mice injected with unselected cells showed one tumor out of six injections with 25,000 cells (17%). Injection of lower cell numbers did not lead to tumor formation. CD98^{low} cell fractions did not result in any tumor growth, whereas the CD98^{high} population grew out to a tumor in four out of six injections with 25,000 cells (67%, one-tailed p-value = 0.03, two-tailed p-value = 0.06). From these observations we concluded that selection for CD98^{high} cells results in considerable enrichment of cancer initiating cells.

To further investigate whether CD98^{high} cells were capable of giving rise to various progeny lineages, the morphology of the parental tumor was compared to that of the tumors arising from the inoculation of CD98^{high} cells. Tumor morphology was identical and, in addition, the same heterogeneity in CD98 expression could be found as in the parental tumor (Supplementary Fig. S3); both CD98^{high} and CD98^{low} cells could be detected. These newly grown tumors were also passaged through another round of tumor formation by inoculation of 25,000 sorted cells from the CD98^{high}, CD98^{low} and unselected populations. Again, mice injected with CD98^{low} cells did not develop any tumors, whereas CD98^{high} cells developed tumors in five out of ten inoculations (Table 2, two-tailed p-value = 0.04).

Molecular characterization of CD98^{high} population

We showed that the CD98^{high} population is enriched for cancer stem cells that are capable of tumor formation *in vivo*. To further investigate the difference between CD98^{high} and CD98^{low} cells at the molecular level, we isolated these cell populations from four different HNX-OE tumors. We extracted the RNA and analyzed the gene expression using a microarray covering all human genes. Data analysis revealed 292 genes that were expressed at a significantly higher level in the CD98^{high} cells as compared to the CD98^{low} cells (FDR-corrected p-value <0.02, see Supplementary Table S2). We used the STRING database (version 9.0) to find associations between these 292 genes and found that the dataset was significantly enriched for genes that play a role in cell cycle and DNA integrity ($p<1x10^{-13}$, indicated as darker cirkels in Fig. 5A). Furthermore, 387 genes

Table 2. Second serial transplantation of 25,000 CD98^{high}, CD98^{low} and unselected HNX-OE cells in NOD/SCID IL2Rγ^{null} mice.

Population	No. tumors/no. injections	Days to first palpability
CD98^{high}	5/10	39±3
CD98^{low}	0/8	NA
Unselected	3/8	39

Abbreviation: NA, not applicable

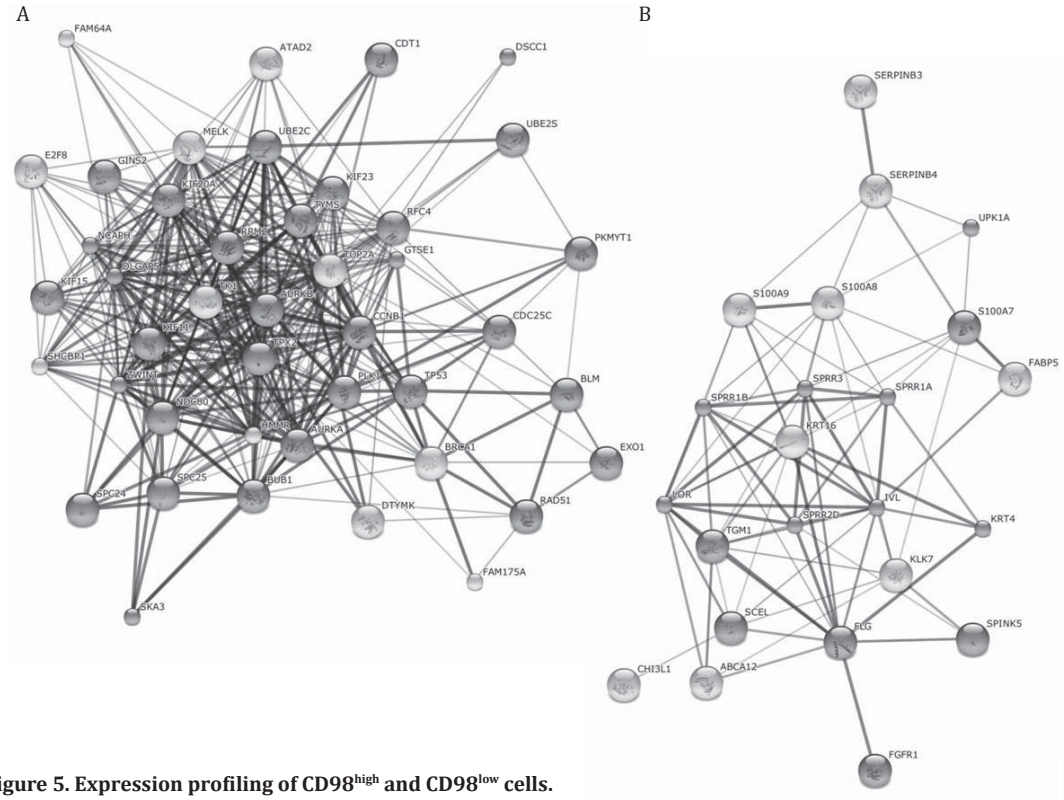

Figure 5. Expression profiling of CD98^{high} and CD98^{low} cells.
(A) STRING mediated clustering of the genes that are expressed at a significantly higher level in CD98^{high} cells as compared to CD98^{low} cells (FDR-corrected p-value <0.02) resulted in one large cluster, mainly containing genes involved in cell cycle regulation and DNA integrity (indicated in dark grey). The cluster is displayed in 'confidence view'; stronger associations between indicated genes are represented with thicker lines. (B) Clustering of the genes that are expressed at a significantly higher level in CD98^{low} cells as compared to CD98^{high} cells (FDR-corrected p-value <0.02) formed a cluster containing many genes that play a role in tissue differentiation. Several genes described to be important in keratinocyte differentiation in particular were present in this cluster (shown in dark grey). In this 'confidence view' thicker lines represent stronger associations.

showed significantly higher expression in the CD98^{low} cells as compared to the CD98^{high} cells (FDR-corrected p-value <0.02, see Supplementary Table S3). We again consulted the STRING database, which showed a cluster (Fig. 5B) containing many proteins specifically involved in cellular differentiation, including keratinocyte differentiation ($p=2.27x10^{-10}$, shown in dark grey).

DISCUSSION

Over the past decade, head and neck cancer is increasingly treated with chemoradiation protocols, but the variation in treatment response is a major concern. Many studies searched in vain for cellular characteristics that can be used as good predictive markers for tumor response, but the identification of the CSCs as a treatment resistant subpopulation of tumor cells provided new directions for exploration. Since CSCs are responsible for the maintenance of all cells in the tumor, a treatment specifically targeting the CSC population seems the most effective way to eradicate a tumor. New challenges lie in the characterization and isolation of these CSCs. So far, CD44 has been the most frequently used marker for squamous cancer stem cells[12,19-23].
The heterodimeric glycoprotein CD98 has been implicated in immunity as well as in cancer. Expression of the CD98 heavy chain or light chain has been investigated with respect to clinical prognosis of multiple tumor types[24-31]. Nearly all studies report higher CD98 expression in

progressive and metastatic tumors, which relates to a poor prognosis. Overexpression of CD98 drives both anchorage independence and tumorigenesis[32,33], but the mechanism behind this is not clear. It has been shown that the CD98 heavy chain mediates increased integrin signaling[34], leading to AKT phosphorylation[35] and eventually to stimulation of cell survival, anchorage-independence and metastasis. Furthermore, the CD98 light chain (LAT-1 or LAT-2) is able to import essential amino acids[36], which in turn can activate the mTOR pathway. This leads to promotion of cell growth, proliferation and protein synthesis. Thus, CD98 is important in cancer, probably mediated through increased amino acid transport and stimulation of integrin signaling.

Here we present data on the application of CD98 as a marker for the isolation of a cancer stem cell enriched fraction in HNSCC. CD98 expression is basal cell-specific, it enriches for the cancer stem cell population when tested in mouse models, and the protein is resistant to the enzymatic protocols used to generate single cell suspensions from solid tumors. CD98 antibodies are commercially available and allow immunostaining of formalin-fixed paraffin-embedded tissues as well as FACS analysis. We were not able to make a direct comparison between CD98 and CD44, as CD44 is for some reason very sensitive to proteolytic degradation on the VU-SCC-OE model. Future experiments in other models or primary tumors would allow to make such comparisons between CD98 and the more established CSC marker CD44.

One of the characteristics of CSCs is the ability to self-renew. Expression profiling of the $CD98^{high}$ tumor fraction revealed higher mRNA expression of cell cycle associated genes as compared to the $CD98^{low}$ cells. It seems that CSCs tightly regulate cell cycle progression, more specifically the moment of cell division (via genes like *PLK1* and *TP53*), as well as the process of cell division. Many genes that are differentially expressed in $CD98^{high}$ cells are involved in proper assembly of the mitotic spindle and chromosome segregation. Examples of such genes are the aurora kinases A and B, *TPX2* and *KIF11*. Also expression of genes responsible for maintenance of DNA integrity was high in these cells, implicating the importance of strict control mechanisms in the cells that fuel the tumor bulk. The $CD98^{low}$ cells showed increased expression of genes involved in cellular differentiation when compared to the $CD98^{high}$ cells. Genes specifically involved in keratinization, like members of the SPRR family[37], were found to be highly expressed in the $CD98^{low}$ subpopulation. This result can be easily correlated to our finding that none of the inoculations with $CD98^{low}$ cells resulted in the formation of a tumor, implicating that $CD98^{low}$ cells are presumably already differentiated and therefore incapable of producing progeny. Stem cell related genes, like *OCT4*, *KLF4*, *SOX2* and *Nanog*, did not display significant differences when we compared $CD98^{high}$ versus $CD98^{low}$ cell populations.

In summary, our data again show that head and neck cancer is a heterogeneous disease, not only between tumors but also intratumorally. This once more shows the importance of identifying and eradicating all different cell populations within an established tumor in order to cure the disease. Therefore detailed characterization of the different cell populations is urgently awaited.

ACKNOWLEDGEMENTS

This study was performed within the framework of CTMM, the Centre for Translational Molecular Medicine. AIRFORCE project (grant 03O-103).

Supplementary Fig. S1. Knockdown of CD98 or TACSTD2 does not alter the cellular phenotype.
UM-SCC-11B cells were transfected with siRNA pools targeting TACSTD2, CD98HC, CD98LC or a combination of CD98HC and CD98LC. The phenotype of the cells did not change after knockdown of the mRNA sequences targeted by the siRNAs as compared with a culture transfected with the non-targeting siCONTROL or the untransfected parental culture. Pictures were taken with a 10x magnification.

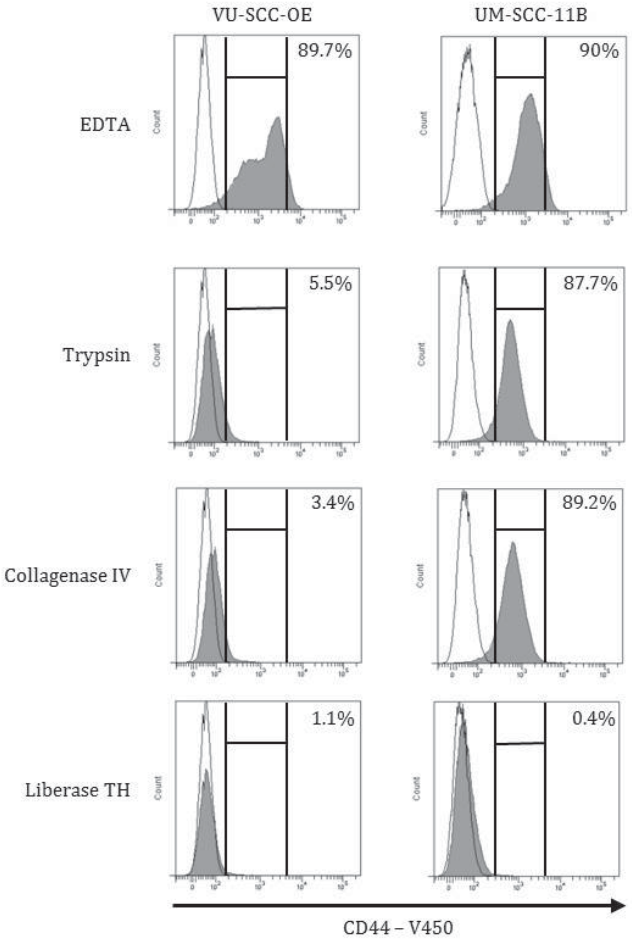

Supplementary Fig. S2. CD44v6 expression after proteolytic treatment.
VU-SCC-OE (left) and UM-SCC-11B (right) cells were harvested as indicated in Fig. 4 and CD44 expression was analyzed by flow cytometry. EDTA treatment was used as a positive control. White peaks represent negative control measurements and CD44 expression is represented by black peaks. Ninety percent of the events were gated in the EDTA control measurement. Figures are representative for at least duplicate experiments.

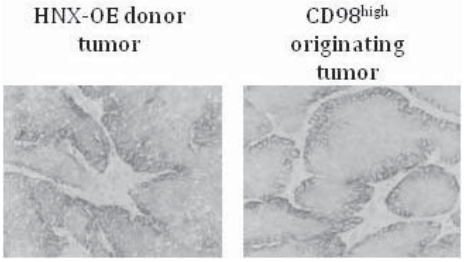

Supplementary Fig. S3. CD98^{high} cell originating xenografts resemble parental tumor.
CD98 expression in the parental tumor (left) and a tumor arising from inoculated CD98^{high} cells (right). Both tumors show CD98-positive and CD98-negative cells, indicating that CD98^{high} cells can also give rise to a CD98-negative cell lineage after tumor outgrowth. Furthermore, the tumors show the same morphological characteristics. Pictures were taken with a 20x magnification.

Supplementary Table S1. Take rate unselected VU-SCC-OE cells in nu/nu mice and NOD/SCID IL2Rγ^{null} mice.

Mouse model	No. tumors/no. injections					
	Cells injected					
	2,500,000	250,000	25,000	2,500	250	25
Nu/nu	12/12	10/12	6/12	0/12	0/12	ND
NOD/SCID IL2Rγ^{null}	11/12	11/12	7/12	8/12	4/12	1/14

Abbreviation: ND, not determined

Supplementary Table S2. 292 genes are expressed at a significantly higher level in the CD98^{high} cells as compared to the CD98^{low} cells.

GeneName	Systematic Name	logFC	Adjusted p-value	GeneName	Systematic Name	logFC	Adjusted p-value
ANXA10	NM_007193	1.78E+14	0.0174	CB123670	CB123670	0.922953	0.0149
IGFBP7	NM_001553	1.43E+14	0.0136	GLIPR1	NM_006851	0.917912	0.0195
CAV1	NM_001753	1.38E+14	0.0136	LOXL2	NM_002318	0.904898	0.0165
CCL5	NM_002985	1.31E+14	0.0174	VEGFC	NM_005429	0.903614	0.0149
SULT1E1	NM_005420	1.26E+14	0.0166	GAL	NM_015973	0.903149	0.0174
MMP1	NM_002421	1.22E+14	0.0174	CMTM7	NM_138410	0.90192	0.0174
FHOD3	NM_025135	1.19E+14	0.0136	A_24_P306896	A_24_P306896	0.898125	0.0174
ADRA1B	NM_000679	1.18E+14	0.0173	RGS20	NM_170587	0.893196	0.0173
WDR66	NM_144668	1.16E+14	0.0140	IL7R	NM_002185	0.88	0.0174
CTNNAL1	NM_003798	1.13E+14	0.0136	FGFBP1	NM_005130	0.883747	0.0144
BC018597	BC018597	1.12E+14	0.0140	LTBP1	NM_206943	0.883639	0.0140
THC2657193	THC2657193	1.11E+14	0.0136	FEZ1	NM_005103	0.87563	0.0165
NT5E	NM_002526	1.09E+14	0.0174	SNCA	NM_007308	0.869826	0.0174
AL833309	AL833309	1.06E+14	0.0165	FLRT2	NM_013231	0.867833	0.0174
CDH13	NM_001257	1.06E+14	0.0144	CAV3	NM_001234	0.861227	0.0165
IL1B	NM_000576	1.06E+14	0.0176	DPY19L1	NM_015283	0.849636	0.0166
LHFP	NM_005780	1.04E+14	0.0136	CCDC74B	NM_207310	0.84748	0.0149
FYB	NM_001465	1.04E+14	0.0174	CBS	NM_000071	0.838627	0.0192
FJX1	NM_014344	1E+14	0.0136	COTL1	NM_021149	0.835236	0.0163
SLC7A5	NM_003486	5.89E+13	0.0193	EFEMP1	NM_004105	0.835068	0.0136
COL17A1	NM_000494	5.46E+13	0.0166	COL4A2	NM_001846	0.834753	0.0137
CCDC3	NM_031455	0.992342	0.0140	PAQR8	NM_133367	0.834501	0.0150
NOV	NM_002514	0.966253	0.0136	RADIL	NM_018059	0.81927	0.0137
ASPHD2	AK097157	0.952386	0.0174	KIRREL	AK090554	0.797205	0.0159
LRRC38	CR622769	0.943729	0.0186	A_24_P50328	A_24_P50328	0.77842	0.0165
DFNA5	NM_004403	0.931206	0.0144	BC032716	BC032716	0.777745	0.0174

Continued: Supplementary Table S2. 292 genes are expressed at a significantly higher level in the CD98^{high} cells as compared to the CD98^{low} cells.

GeneName	Systematic Name	logFC	Adjusted p-value	GeneName	Systematic Name	logFC	Adjusted p-value
CD38	NM_001775	0.77	0.0166	S73202	S73202	0.628333	0.0160
COL12A1	NM_004370	0.767628	0.0160	SYT13	NM_020826	0.626392	0.0165
PDPN	NM_198389	0.767154	0.0165	MPHOSPH1	NM_016195	0.623535	0.0188
C10orf67	NM_153714	0.765951	0.0186	A_32_P153361	A_32_P153361	0.62299	0.0186
ELAVL2	NM_004432	0.764959	0.0149	RAI14	NM_015577	0.619512	0.0174
DDAH1	NM_012137	0.763847	0.0177	DKK1	NM_012242	0.618944	0.0151
CYP26B1	NM_019885	0.762716	0.0165	ICAM1	NM_000201	0.614857	0.0195
A_23_P28927	A_23_P28927	0.759122	0.0195	CD69	NM_001781	0.613774	0.0198
LOC129293	NM_001080824	0.758304	0.0186	AV749257	AV749257	0.61332	0.0180
WNT10A	NM_025216	0.754046	0.0147	ZNF469	AB058761	0.610085	0.0174
ARHGEF10	NM_014629	0.751096	0.0174	LOC341230	XR_018617	0.60722	0.0195
C9orf21	NM_153698	0.749796	0.0199	RAC2	NM_002872	0.60213	0.0169
COL4A1	NM_001845	0.746155	0.0192	SLC39A14	NM_015359	0.60	0.0174
LAMC2	NM_018891	0.743466	0.0174	FGF13	NM_004114	0.59954	0.0188
IFIT3	NM_001549	0.737836	0.0166	AURKB	NM_004217	0.593607	0.0166
CAV2	NM_001233	0.737795	0.0188	PRDM13	NM_021620	0.587502	0.0193
BM973227	BM973227	0.735135	0.0177	LRRC8C	NM_032270	0.585521	0.0174
MNS1	NM_018365	0.731977	0.0195	IKIP	NM_201612	0.582483	0.0174
DLL1	NM_005618	0.72	0.0140	UBD	NM_006398	0.581286	0.0166
MOBKL2B	NM_024761	0.719043	0.0174	CDCA7	NM_031942	0.580501	0.0174
HSPA12A	NM_025015	0.713972	0.0166	AW972815	AW972815	0.579118	0.0174
SORBS1	NM_001034954	0.712722	0.0174	C11orf82	NM_145018	0.577746	0.0191
NRP2	NM_201266	0.706273	0.0166	MPV17L	NM_173803	0.577394	0.0165
SLC1A3	NM_004172	0.704731	0.0174	MTHFD1L	NM_015440	0.573841	0.0166
DLX1	NM_178120	0.704023	0.0144	A_24_P367100	A_24_P367100	0.573055	0.0174
OASL	NM_003733	0.702853	0.0144	C3	NM_000064	0.572965	0.0166
U79293	U79293	0.697532	0.0188	UBE2C	NM_181803	0.569558	0.0176
FOXA2	NM_021784	0.696115	0.0197	HPSE	NM_006665	0.56938	0.0174
CYR61	NM_001554	0.694331	0.0160	SLC1A4	NM_003038	0.56797	0.0166
AF131762	AF131762	0.692534	0.0174	DST	NM_001723	0.567878	0.0173
AGMAT	NM_024758	0.690415	0.0174	C13orf3	BC013418	0.57	0.0180
SLC2A5	NM_003039	0.689923	0.0150	DSCC1	NM_024094	0.566347	0.0174
A_32_P167212	A_32_P167212	0.685909	0.0166	GSG2	AK056691	0.56059	0.0186
THC2663201	THC2663201	0.680253	0.0174	CDC25C	NM_001790	0.558299	0.0166
AREG	NM_001657	0.676674	0.0178	THC2603089	THC2603089	0.55823	0.0176
MXRA5	NM_015419	0.67615	0.0174	ZNF215	NM_013250	0.55553	0.0187
FAM54A	NM_138419	0.669811	0.0149	MELK	NM_014791	0.554249	0.0174
A_24_P67494	A_24_P67494	0.664669	0.0197	EPB41L2	NM_001431	0.552676	0.0174
KREMEN2	NM_172229	0.662438	0.0159	AA725860	AA725860	0.549688	0.0188
CMTM3	NM_144601	0.661833	0.0193	SPC24	ENST0000 0293743	0.54867	0.0166
FHL1	NM_001449	0.658261	0.0180	TOP2A	NM_001067	0.544784	0.0171
MAP2	NM_002374	0.656134	0.0166	SPC25	NM_020675	0.542794	0.0174
ANK1	NM_000037	0.646889	0.0174	AA234312	AA234312	0.541878	0.0186
BG462058	BG462058	0.633193	0.0149	C14orf145	NM_152446	0.541003	0.0166
AK024926	AK024926	0.630455	0.0149	RRM2	NM_001034	0.535859	0.0195
FSD1	NM_024333	0.628452	0.0177	KIF15	NM_020242	0.535363	0.0173

Continued: Supplementary Table S2. 292 genes are expressed at a significantly higher level in the CD98^{high} cells as compared to the CD98^{low} cells.

GeneName	Systematic Name	logFC	Adjusted p-value	GeneName	Systematic Name	logFC	Adjusted p-value
CD97	NM_078481	0.533973	0.0174	XR_015343	XR_015343	0.489456	0.0186
MYO5A	NM_000259	0.532676	0.0173	FOXM1	NM_202002	0.489038	0.0174
C16orf45	NM_033201	0.53	0.0173	SERINC2	NM_178865	0.488433	0.0195
RPGRIP1L	NM_015272	0.531309	0.0172	NRGN	NM_006176	0.48842	0.0174
CAMK4	NM_001744	0.531022	0.0174	A_24_P7040	A_24_P7040	0.487848	0.0174
THC2560068	THC2560068	0.530447	0.0174	TK1	NM_003258	0.485168	0.0199
TIMP4	NM_003256	0.530409	0.0186	THC2536560	THC2536560	0.484658	0.0187
AURKA	NM_198433	0.528663	0.0174	FAM107B	NM_031453	0.483321	0.0174
THC2540738	THC2540738	0.528525	0.0174	IFITM3	NM_021034	0.48142	0.0174
MLSTD1	NM_018099	0.528034	0.0199	HMGA2	NM_003483	0.479413	0.0197
MYBL1	NM_001080416	0.525375	0.0173	ABCC3	NM_003786	0.478301	0.0174
LAMA3	NM_198129	0.524334	0.0186	HSPB3	NM_006308	0.478202	0.0180
CYP4V2	NM_207352	0.523535	0.0199	TPX2	NM_012112	0.476684	0.0188
POLA2	NM_002689	0.520563	0.0193	ODC1	NM_002539	0.475976	0.0174
MAPRE2	NM_014268	0.520083	0.0188	IL1RAP	NM_002182	0.475432	0.0195
MET	NM_000245	0.519666	0.0174	THC2497780	THC2497780	0.474796	0.0174
PLEK2	NM_016445	0.519663	0.0197	ZNF488	ENST0000 0298129	0.47	0.0174
EXO1	NM_003686	0.519414	0.0174	KIF20A	NM_005733	0.471213	0.0174
NANOS1	NM_199461	0.519214	0.0174	RAD51	NM_002875	0.470908	0.0174
CDCA2	NM_152562	0.518682	0.0174	ERAP2	NM_022350	0.469944	0.0188
TPM1	NM_001018004	0.518253	0.0174	PKMYT1	NM_004203	0.468657	0.0180
BLM	NM_000057	0.517422	0.0174	FBXO5	NM_012177	0.467831	0.0176
LAMC1	NM_002293	0.517336	0.0176	SERPINE2	NM_006216	0.467569	0.0187
VAV2	NM_003371	0.515562	0.0186	MND1	NM_032117	0.467503	0.0174
EMILIN2	NM_032048	0.514585	0.0174	GALNT2	NM_004481	0.466956	0.0186
MTBP	NM_022045	0.5143	0.0174	CXCL2	NM_002089	0.465368	0.0187
THC2645710	THC2645710	0.514079	0.0174	THAP10	NM_020147	0.461061	0.0195
AL832534	AL832534	0.513947	0.0173	NCAPG	NM_022346	0.459025	0.0188
GALNT12	NM_024642	0.513209	0.0198	SHCBP1	NM_024745	0.458441	0.0174
XR_018907	XR_018907	0.511993	0.0174	CD320	NM_016579	0.457433	0.0181
DRAM	NM_018370	0.509834	0.0174	GTSE1	NM_016426	0.456125	0.0199
TGFBR2	NM_001024847	0.507801	0.0174	FANCI	NM_018193	0.45466	0.0185
BAIAP2L2	NM_025045	0.507314	0.0174	NCAPH	NM_015341	0.454092	0.0199
UPP1	NM_181597	0.506268	0.0176	CRTAP	NM_006371	0.450173	0.0177
ENST0000 0285605	ENST0000 0285605	0.504008	0.0174	ITGA6	NM_000210	0.45	0.0187
PRKCDBP	NM_145040	0.501481	0.0174	AW939027	AW939027	0.448227	0.0185
THC2672257	THC2672257	0.50101	0.0196	SLC7A1	NM_003045	0.448226	0.0177
BRCA1	NM_007295	0.497977	0.0188	THC2668815	THC2668815	0.447286	0.0187
SLC6A2	NM_001043	0.497759	0.0197	ENST0000 0335534	ENST0000 0335534	0.445999	0.0184
FHL2	NM_001039492	0.49683	0.0174	CD302	NM_014880	0.443013	0.0187
LOC493869	NM_001008397	0.49498	0.0196	SPECC1	NM_152904	0.442298	0.0177
IFITM2	NM_006435	0.494289	0.0177	A_32_P158376	A_32_P158376	0.44165	0.0195
NDC80	NM_006101	0.49	0.0186	KIF23	NM_138555	0.43983	0.0191
FOXF2	NM_001452	0.493163	0.0188	CARD10	NM_014550	0.43922	0.0192

Continued: Supplementary Table S2. 292 genes are expressed at a significantly higher level in the CD98^{high} cells as compared to the CD98^{low} cells.

GeneName	Systematic Name	logFC	Adjusted p-value	GeneName	Systematic Name	logFC	Adjusted p-value
FAS	NM_000043	0.438934	0.0180	SLC35F3	NM_173508	0.41	0.0188
POLQ	NM_199420	0.438252	0.0195	ENST0000 0376793	ENST0000 0376793	0.404465	0.0188
AMIGO2	NM_181847	0.43763	0.0176	C9orf100	NM_032818	0.403889	0.0195
A_23_P123234	A_23_P123234	0.434983	0.0199	CDR2	NM_001802	0.402138	0.0199
CCNB1	NM_031966	0.431369	0.0195	UBE2S	NM_014501	0.401846	0.0195
C15orf23	ENST0000 0249776	0.430854	0.0177	THBS2	L12350	0.401819	0.0199
THC2534530	THC2534530	0.429998	0.0188	TCF19	NM_007109	0.401244	0.0195
FAM64A	NM_019013	0.42711	0.0187	A_32_P17672	A_32_P17672	0.400845	0.0197
KLHL23	NM_144711	0.426892	0.0186	KPNA2	NM_002266	0.40066	0.0192
MAMLD1	NM_005491	0.426578	0.0199	UBE2T	NM_014176	0.400477	0.0193
FKBP11	NM_016594	0.425641	0.0187	THC2568453	THC2568453	0.399285	0.0193
PXN	NM_002859	0.425568	0.0195	ZWINT	NM_032997	0.396798	0.0195
CDCA8	NM_018101	0.42544	0.0199	MCM2	NM_004526	0.396282	0.0195
BUB1	NM_004336	0.423598	0.0188	RFC4	NM_002916	0.392053	0.0193
E2F8	NM_024680	0.422169	0.0195	ACOT9	NM_001037171	0.391144	0.0188
XR_017068	XR_017068	0.420506	0.0195	ITGB1	NM_002211	0.390385	0.0192
XR_019510	XR_019510	0.420345	0.0192	ATAD2	NM_014109	0.388722	0.0198
KLHL13	NM_033495	0.419649	0.0195	MT1B	NM_005947	0.386695	0.0195
HMMR	NM_012484	0.419094	0.0187	LMNB2	NM_032737	0.39	0.0198
BC041955	BC041955	0.41762	0.0198	DLG7	NM_014750	0.38505	0.0199
PPP1R14C	NM_030949	0.417103	0.0197	CDT1	NM_030928	0.38355	0.0195
POLR1E	NM_022490	0.416973	0.0187	TP53	NM_000546	0.383133	0.0195
PLK1	NM_005030	0.413319	0.0195	ADORA2B	NM_000676	0.381496	0.0199
THC2655811	THC2655811	0.41206	0.0199	CCDC98	NM_139076	0.38101	0.0195
AP2B1	NM_001030006	0.411969	0.0187	NELF	NM_015537	0.379462	0.0195
TMEM194	NM_015257	0.411022	0.0199	C1orf112	NM_018186	0.378426	0.0195
RUVBL1	NM_003707	0.41012	0.0198	AK021874	AK021874	0.377481	0.0199
TINAGL1	NM_022164	0.407661	0.0195	GINS2	NM_016095	0.37469	0.0195
TYMS	NM_001071	0.407265	0.0187	PTRF	NM_012232	0.371618	0.0199
KIF11	NM_004523	0.40663	0.0198	GALNT14	NM_024572	0.367693	0.0199

Supplementary Table S3. 387 genes are expressed at a significantly higher level in the CD98^{low} cells as compared to the CD98^{high} cells.

GeneName	Systematic Name	logFC	Adjusted p-value	GeneName	Systematic Name	logFC	Adjusted p-value
CRCT1	NM_019060	-1.8E+14	0.0136	MGC23985	NM_206966	-1.1E+14	0.0199
S100A8	NM_002964	-1.8E+14	0.0140	CST6	NM_001323	-1.1E+14	0.0136
SPRR2G	NM_001014291	-1.7E+14	0.0136	APOBEC3A	NM_145699	-1.1E+14	0.0166
SPRR3	NM_005416	-1.7E+14	0.0136	IGFBP5	NM_000599	-1.1E+14	0.0136
TACR3	NM_001059	-1.7E+14	0.0174	CEACAM5	NM_004363	-1.1E+14	0.0174
S100A7	NM_002963	-1.7E+14	0.0136	SLC24A3	NM_020689	-1.1E+14	0.0149
A_24_P932270	A_24_P932270	-1.7E+14	0.0174	IVL	NM_005547	-1.1E+14	0.0140
PROM1	NM_006017	-1.7E+14	0.0174	ENST00000 0399048	ENST00000 0399048	-1.1E+14	0.0136
KCNE4	NM_080671	-1.6E+14	0.0136	CLCA4	NM_012128	-1E+14	0.0198
GREB1	NM_148903	-1.6E+14	0.0188	KRT80	NM_182507	-1E+14	0.0144
PYHIN1	BC020822	-1.5E+14	0.0136	TXNIP	NM_006472	-1E+14	0.0136
IGFL2	NM_001002915	-1.5E+14	0.0144	LOC645638	XR_040455	-1E+14	0.0140
CRNN	NM_016190	-1.5E+14	0.0174	FUT3	NM_000149	-1E+14	0.0146
SPRR2D	NM_006945	-1.5E+14	0.0147	LOR	NM_000427	-6.2E+13	0.0136
COL15A1	NM_001855	-1.5E+14	0.0176	CYP2C19	NM_000769	-6E+13	0.0174
KLK12	NM_145894	-1.4E+14	0.0136	FARP1	NM_005766	-5.4E+13	0.0140
HSD17B2	NM_002153	-1.4E+14	0.0136	CGNL1	NM_032866	-5.4E+13	0.0136
THC2553238	THC2553238	-1.4E+14	0.0159	SPINK6	NM_205841	-1.9E+13	0.0136
C15orf48	NM_032413	-1.4E+14	0.0147	CPN2	NM_001080513	-1.2E+13	0.0188
A_24_P290087	A_24_P290087	-1.4E+14	0.0136	CYP3A4	NM_017460	-0.9952	0.0174
LCE3D	NM_032563	-1.4E+14	0.0136	SPARCL1	NM_004684	-0.99512	0.0150
KRTDAP	NM_207392	-1.4E+14	0.0140	THC2708669	THC2708669	-0.993	0.0136
RGS5	NM_003617	-1.4E+14	0.0174	CD24	L33930	-0.98646	0.0144
KRT16	NM_005557	-1.4E+14	0.0136	KRT23	NM_015515	-0.98068	0.0192
A_23_P247	A_23_P247	-1.4E+14	0.0159	BX413550	BX413550	-0.97951	0.0174
CDH16	NM_004062	-1.3E+14	0.0136	SPINK1	NM_003122	-0.9774	0.0192
SPRR2C	NR_003062	-1.3E+14	0.0173	SOBP	NM_018013	-0.96649	0.0136
CD36	S67044	-1.3E+14	0.0136	SPNS2	NM_001124758	-0.96047	0.0136
FLG	NM_002016	-1.3E+14	0.0195	RDH12	NM_152443	-0.95292	0.0177
PROS1	NM_000313	-1.3E+14	0.0146	THC2634862	THC2634862	-0.95065	0.0177
SPRR1A	NM_005987	-1.3E+14	0.0149	RORA	NM_134260	-0.94565	0.0140
THC2671679	THC2671679	-1.3E+14	0.0136	KRT4	NM_002272	-0.94533	0.0142
ANKRD35	NM_144698	-1.2E+14	0.0136	CLIC3	NM_004669	-0.94343	0.0165
S100A9	NM_002965	-1.2E+14	0.0173	SPINK5	NM_006846	-0.94256	0.0174
CEACAM6	BC005008	-1.2E+14	0.0174	TMPRSS11F	NM_207407	-0.94209	0.0140
NOS2A	NM_000625	-1.2E+14	0.0136	DHRS9	NM_005771	-0.93015	0.0140
ICEBERG	NM_021571	-1.2E+14	0.0195	ARHGAP24	AK130576	-0.92823	0.0147
CYP2C18	NM_000772	-1.2E+14	0.0174	TFF3	NM_003226	-0.92706	0.0140
BI026064	BI026064	-1.2E+14	0.0136	AI620901	AI620901	-0.92388	0.0140
SCEL	NM_144777	-1.2E+14	0.0174	AQP5	BC032946	-0.92166	0.0136
SPRR1B	NM_003125	-1.2E+14	0.0174	TTC9	NM_015351	-0.91924	0.0186
KCNJ1	NM_153767	-1.2E+14	0.0136	KCNH5	NM_172376	-0.91546	0.0177
LOC646486	NM_001105281	-1.1E+14	0.0173	WNT5A	NM_003392	-0.91515	0.0160
SLC6A14	NM_007231	-1.1E+14	0.0195	C1orf165	NM_024603	-0.90418	0.0187
A_24_P548966	A_24_P548966	-1.1E+14	0.0136	FUT5	NM_002034	-0.90207	0.0136
GPR128	NM_032787	-1.1E+14	0.0140	ADH1A	NM_000667	-0.90015	0.0141

Continued: Supplementary Table S3. 387 genes are expressed at a significantly higher level in the CD98^{low} cells as compared to the CD98^{high} cells.

GeneName	Systematic Name	logFC	Adjusted p-value	GeneName	Systematic Name	logFC	Adjusted p-value
SDR-O	NM_148897	-0.90	0.0195	UPK1A	NM_007000	-0.75	0.0174
CEACAM7	NM_006890	-0.89162	0.0174	GDA	NM_004293	-0.74689	0.0143
A_24_P174353	A_24_P174353	-0.89116	0.0187	CHI3L1	NM_001276	-0.74679	0.0140
TMEM45B	NM_138788	-0.89	0.0174	IL10RA	NM_001558	-0.74641	0.0174
A_32_P224040	A_32_P224040	-0.88413	0.0136	TAF9B	NM_015975	-0.74477	0.0174
OSTalpha	NM_152672	-0.87415	0.0199	TMEM125	NM_144626	-0.7435	0.0140
ADAM19	NM_033274	-0.87317	0.0140	WFIKKN1	NM_053284	-0.73943	0.0173
SPRR2E	NM_001024209	-0.87045	0.0166	NTF3	NM_002527	-0.73227	0.0186
A_32_P119949	A_32_P119949	-0.86936	0.0136	GLYATL2	NM_145016	-0.73061	0.0185
THC2649467	THC2649467	-0.86929	0.0174	MGC2780	BC004179	-0.72954	0.0186
ZNF322A	NM_024639	-0.86694	0.0136	LUM	NM_002345	-0.72811	0.0173
LOC283666	BC048264	-0.8642	0.0136	DNASE1L2	NM_001374	-0.72474	0.0166
PGLYRP4	NM_020393	-0.85479	0.0136	BM768581	BM768581	-0.72469	0.0195
LONRF2	NM_198461	-0.85163	0.0174	ADH7	NM_000673	-0.72248	0.0173
LOC374569	NM_001080464	-0.8459	0.0195	SULT2B1	NM_004605	-0.72072	0.0188
DAPL1	NM_001017920	-0.84533	0.0152	RASGRP1	NM_005739	-0.72013	0.0167
LIPH	NM_139248	-0.84125	0.0182	RRAD	NM_004165	-0.71812	0.0136
SERPINB3	NM_006919	-0.83641	0.0195	VWF	NM_000552	-0.71687	0.0149
ICAM4	NM_001544	-0.83	0.0174	CA13	NM_198584	-0.72	0.0140
ABCA12	NM_173076	-0.83151	0.0169	KLK7	NM_005046	-0.71555	0.0177
SMPD3	NM_018667	-0.8291	0.0166	RASGRP2	NM_153819	-0.71538	0.0159
THC2672319	THC2672319	-0.82803	0.0166	ROPN1	NM_017578	-0.70677	0.0140
BNIPL	NM_138278	-0.8268	0.0177	SDCBP2	NM_080489	-0.70613	0.0144
AF113013	AF113013	-0.81813	0.0136	FAM80A	NM_173642	-0.69439	0.0140
GDPD3	NM_024307	-0.81568	0.0140	BAI1	NM_001702	-0.69246	0.0144
FAM3D	NM_138805	-0.81505	0.0136	BMP3	NM_001201	-0.69142	0.0166
SPAG17	NM_206996	-0.81373	0.0140	ELN	NM_000501	-0.68973	0.0144
SERPINB4	NM_002974	-0.81068	0.0188	PARM1	NM_015393	-0.68971	0.0195
ZNF322B	NM_199005	-0.80571	0.0137	PGLYRP3	NM_052891	-0.68919	0.0188
KIAA1683	NM_025249	-0.79999	0.0140	SEPP1	NM_005410	-0.68405	0.0166
PSCA	NM_005672	-0.79995	0.0140	C21orf67	AY040088	-0.68077	0.0151
GSTA1	NM_145740	-0.7996	0.0140	ALDH1A1	NM_000689	-0.67685	0.0144
LY6G6C	NM_025261	-0.79948	0.0180	RASSF5	NM_182664	-0.67595	0.0199
SKAP1	NM_003726	-0.7899	0.0146	SEMA5A	NM_003966	-0.67572	0.0195
ENST0000 0343959	ENST0000 0343959	-0.78183	0.0166	DSC2	NM_024422	-0.6703	0.0197
ID2	NM_002166	-0.78095	0.0136	KIAA1244	NM_020340	-0.66808	0.0174
ABCA3	NM_001089	-0.77328	0.0144	SNX31	NM_152628	-0.66745	0.0174
CDH22	NM_021248	-0.77147	0.0174	PLXDC2	NM_032812	-0.66726	0.0174
CEL	NM_001807	-0.77039	0.0165	MUC20	NM_152673	-0.66644	0.0147
GSTA5	NM_153699	-0.76832	0.0174	CCL17	NM_002987	-0.66384	0.0176
GSTA2	NM_000846	-0.76671	0.0136	RGL1	NM_015149	-0.66209	0.0199
THC2778165	THC2778165	-0.76537	0.0176	NEBL	NM_006393	-0.66067	0.0195
ADH1C	NM_000669	-0.75973	0.0140	GRAMD1C	NM_017577	-0.6569	0.0161
FGFR1	NM_023110	-0.75717	0.0166	C6orf25	NM_138273	-0.65067	0.0165
TNNT2	NM_000364	-0.75516	0.0137	SASH1	NM_015278	-0.64569	0.0165
SNIP	NM_025248	-0.75331	0.0159	P2RY1	NM_002563	-0.64506	0.0173

Continued: Supplementary Table S3. 387 genes are expressed at a significantly higher level in the CD98^{low} cells as compared to the CD98^{high} cells.

GeneName	Systematic Name	logFC	Adjusted p-value	GeneName	Systematic Name	logFC	Adjusted p-value
CCDC64B	AL833749	-0.64	0.0166	ENST0000 0399865	ENST0000 0399865	-0.55	0.0166
MAFB	NM_005461	-0.63582	0.0149	FAM13A1	NM_014883	-0.55409	0.0166
KIAA1324	AY358366	-0.63537	0.0174	OR7E156P	NR_002171	-0.55407	0.0199
THC2713067	THC2713067	-0.6322	0.0197	IRX6	NM_024335	-0.55358	0.0166
A_23_P33773	A_23_P33773	-0.62861	0.0174	CA392903	CA392903	-0.55074	0.0166
PON3	NM_000940	-0.62707	0.0171	BX647987	BX647987	-0.54834	0.0174
MB	NM_203377	-0.62556	0.0174	LMO7	NM_005358	-0.54724	0.0174
C11orf16	NM_020643	-0.62219	0.0159	RARRES1	NM_002888	-0.54681	0.0176
CTRB2	NM_001025200	-0.62161	0.0174	SOX4	NM_003107	-0.54071	0.0178
RAB3B	AK002107	-0.62134	0.0165	ARHGAP30	NM_001025598	-0.53799	0.0176
CYP1B1	NM_000104	-0.61552	0.0183	C15orf52	NM_207380	-0.53739	0.0174
AK023391	AK023391	-0.61407	0.0180	AL834280	AL834280	-0.53726	0.0166
CACNA2D1	NM_000722	-0.61295	0.0173	CAMK2B	NM_172082	-0.53524	0.0174
FAM139A	NM_173678	-0.61232	0.0195	AK023526	AK023526	-0.53228	0.0174
CPAMD8	NM_015692	-0.61139	0.0174	LOC441461	BC030123	-0.53207	0.0199
OR7E91P	NR_002185	-0.61064	0.0173	C3orf58	NM_173552	-0.52787	0.0166
DA727827	DA727827	-0.61	0.0174	WNK4	NM_032387	-0.52729	0.0173
LYPD3	NM_014400	-0.60892	0.0160	S100P	NM_005980	-0.52675	0.0174
OR7E5P	AK055955	-0.61	0.0160	EHF	NM_012153	-0.53	0.0180
MYLIP	NM_013262	-0.60817	0.0173	GBP2	NM_004120	-0.52395	0.0174
PDZK1IP1	NM_005764	-0.60813	0.0176	THC2645080	THC2645080	-0.52383	0.0174
BF572267	BF572267	-0.60772	0.0188	NBPF11	NM_183372	-0.52097	0.0174
TGM1	NM_000359	-0.60707	0.0173	NOXA1	NM_006647	-0.51973	0.0173
SATB1	NM_002971	-0.60649	0.0174	AK000038	AK000038	-0.51954	0.0174
S1PR4	NM_003775	-0.60528	0.0174	A_24_P101072	A_24_P101072	-0.51697	0.0173
GPRIN2	AB011086	-0.60395	0.0166	AIM1L	NM_001039775	-0.51628	0.0174
RRAGD	NM_021244	-0.60383	0.0166	NBPF10	NM_001039703	-0.5144	0.0173
A2ML1	NM_144670	-0.60281	0.0174	C1orf161	NM_152367	-0.51296	0.0188
SERPINB13	NM_012397	-0.6011	0.0173	ANKRD22	NM_144590	-0.51285	0.0177
CR590573	CR590573	-0.59937	0.0173	NBPF3	NM_032264	-0.51153	0.0174
VLDLR	NM_003383	-0.59909	0.0173	LOC126147	NM_145807	-0.51126	0.0187
LPHN3	NM_015236	-0.59529	0.0166	RALGPS1	NM_014636	-0.51067	0.0174
THC2660361	THC2660361	-0.59326	0.0187	EPS8L1	NM_133180	-0.50765	0.0188
THC2673888	THC2673888	-0.59226	0.0166	ECM1	NM_004425	-0.50694	0.0174
C2orf54	NM_024861	-0.59073	0.0174	XR_018208	XR_018208	-0.50672	0.0174
SPTLC3	NM_018327	-0.59029	0.0174	A_24_P110201	A_24_P110201	-0.50662	0.0173
THC2743491	THC2743491	-0.5888	0.0174	COL9A1	NM_001851	-0.50625	0.0192
LOC100129115	AK095213	-0.58568	0.0166	GRHL3	NM_198173	-0.50602	0.0186
A_23_P96035	A_23_P96035	-0.5854	0.0174	IKZF2	NM_001079526	-0.50499	0.0174
THC2721275	THC2721275	-0.5802	0.0174	LOC100137047-PLA2G4B	NM_005090	-0.50402	0.0174
NR4A2	NM_006186	-0.57838	0.0165	AK001089	AK001089	-0.50339	0.0174
AF318321	AF318321	-0.5757	0.0173	ZBTB20	BC010934	-0.50304	0.0187
TMPRSS13	CR613669	-0.57394	0.0173	THC2682319	THC2682319	-0.5002	0.0174
GSTA3	NM_000847	-0.57039	0.0174	38596	NM_002688	-0.49789	0.0174
AW772196	AW772196	-0.55962	0.0199	PCP4L1	NM_001102566	-0.49774	0.0188
RASAL1	NM_004658	-0.55888	0.0166	A_24_P660797	A_24_P660797	-0.49624	0.0187

Continued: Supplementary Table S3. 387 genes are expressed at a significantly higher level in the CD98^{low} cells as compared to the CD98^{high} cells.

GeneName	Systematic Name	logFC	Adjusted p-value
CEACAM1	NM_001024912	-0.49	0.0174
THC2624264	THC2624264	-0.49425	0.0191
SPRY2	NM_005842	-0.49314	0.0188
NBPF20	NM_001037675	-0.49255	0.0185
A_32_P93584	A_32_P93584	-0.49031	0.0195
MC1R	NM_002386	-0.48942	0.0174
DUSP13	NM_001007271	-0.48939	0.0174
CNKSR3	NM_173515	-0.48453	0.0196
GOLGA8A	NM_181077	-0.48437	0.0188
A_32_P231143	A_32_P231143	-0.48399	0.0176
RP5-1022P6.2	NM_019593	-0.48323	0.0174
OR7E13P	AF238487	-0.4829	0.0188
A_32_P205792	A_32_P205792	-0.48218	0.0174
C17orf55	NM_178519	-0.48174	0.0195
CD517460	CD517460	-0.47952	0.0188
CR612518	CR612518	-0.47886	0.0187
GHR	NM_000163	-0.47831	0.0199
GATM	NM_001482	-0.47736	0.0174
ZDHHC21	NM_178566	-0.48	0.0187
GGT6	NM_153338	-0.47639	0.0195
AJ412029	AJ412029	-0.47599	0.0191
ADAD2	NM_139174	-0.47524	0.0174
THC2663329	THC2663329	-0.47422	0.0180
THC2648851	THC2648851	-0.47373	0.0174
ZNF750	NM_024702	-0.47348	0.0191
CARD14	NM_024110	-0.47129	0.0174
KCNQ1	NM_000218	-0.47122	0.0177
C20orf74	NM_020343	-0.4706	0.0174
LOC645137	ENST0000 0327271	-0.47048	0.0174
THC2704994	THC2704994	-0.47013	0.0174
GPR98	AL136541	-0.4685	0.0177
A26C1A	NM_001083538	-0.4684	0.0186
SEMA3B	NM_004636	-0.4684	0.0177
ERO1LB	NM_019891	-0.46654	0.0187
CYP4F2	NM_001082	-0.46555	0.0174
C3orf57	NM_001040100	-0.46473	0.0174
CR598370	CR598370	-0.4633	0.0174
MXD1	NM_002357	-0.46301	0.0198
A26B3	NM_174981	-0.46237	0.0187
CXorf48	AK123302	-0.46217	0.0174
CR610181	CR610181	-0.46175	0.0174
CHP2	NM_022097	-0.46023	0.0186
LOC387763	NM_001145033	-0.45982	0.0174
A_32_P218707	A_32_P218707	-0.45803	0.0180
EDIL3	NM_005711	-0.45649	0.0174
TLR5	NM_003268	-0.45563	0.0177

GeneName	Systematic Name	logFC	Adjusted p-value
FCGRT	NM_004107	-0.46	0.0188
MUC15	NM_145650	-0.45395	0.0174
BU532663	BU532663	-0.45347	0.0176
AA593970	AA593970	-0.45107	0.0174
A_24_P147849	A_24_P147849	-0.4483	0.0186
PIM1	NM_002648	-0.44532	0.0174
HIST2H2AA4	NM_001040874	-0.44512	0.0174
THC2729353	THC2729353	-0.44432	0.0195
LOC401152	NM_001001701	-0.44421	0.0176
FAM59A	NM_022751	-0.44379	0.0199
THC2607363	THC2607363	-0.44379	0.0195
ARRDC3	NM_020801	-0.44251	0.0190
AK024956	AK024956	-0.44208	0.0186
LRIG1	NM_015541	-0.44075	0.0187
C21orf34	NM_001005732	-0.4401	0.0176
CRYAB	NM_001885	-0.43929	0.0199
hCG_1818231	XR_042007	-0.43763	0.0195
CN294989	CN294989	-0.43759	0.0199
LYG2	NM_175735	-0.44	0.0195
METRNL	NM_001004431	-0.43656	0.0192
C1orf175	NM_001039464	-0.434	0.0187
LOC100134282	AK130705	-0.43316	0.0186
MCF2L	NM_024979	-0.4324	0.0186
BCHE	NM_000055	-0.43148	0.0187
A_24_P655888	A_24_P655888	-0.43121	0.0184
SUSD4	NM_001037175	-0.42887	0.0174
C11orf52	NM_080659	-0.42788	0.0197
EGR1	NM_001964	-0.42778	0.0187
C17orf91	NM_032895	-0.42757	0.0195
DDAH2	NM_013974	-0.42729	0.0188
NUPR1	NM_001042483	-0.42673	0.0186
TCF25	NM_014972	-0.42489	0.0181
LDHD	NM_153486	-0.4236	0.0197
CES2	NM_003869	-0.42179	0.0182
AX721087	AX721087	-0.42164	0.0177
FABP5	NM_001444	-0.41775	0.0176
SFRS18	NM_032870	-0.41731	0.0188
KIFC2	NM_145754	-0.41409	0.0199
TMPRSS2	NM_005656	-0.41318	0.0192
RBM35B	NM_024939	-0.41295	0.0187
HBA1	NM_000558	-0.41273	0.0199
SORT1	NM_002959	-0.41214	0.0188
PCP2	NM_174895	-0.41109	0.0192
ULK1	NM_003565	-0.41012	0.0195
JMY	NM_152405	-0.40921	0.0186
C9orf61	NM_004816	-0.40746	0.0199

Continued: Supplementary Table S3. 387 genes are expressed at a significantly higher level in the CD98^{low} cells as compared to the CD98^{high} cells.

GeneName	Systematic Name	logFC	Adjusted p-value
ZFP36	NM_003407	-0.41	0.0187
PCDH7	NM_032457	-0.40632	0.0190
GPR172B	NM_017986	-0.4062	0.0188
ANK3	AK126851	-0.40615	0.0195
CB162722	CB162722	-0.40482	0.0199
TM7SF2	NM_003273	-0.40472	0.0197
AL833696	AL833696	-0.40375	0.0195
IVNS1ABP	NM_006469	-0.39861	0.0190
PLCB1	NM_015192	-0.39264	0.0188
PPFIBP2	NM_003621	-0.38725	0.0193
KIAA1370	NM_019600	-0.38693	0.0195
ZNF185	NM_007150	-0.38663	0.0195
PAIP2B	NM_020459	-0.38568	0.0199
LOC653391	BC067830	-0.38407	0.0199
RGL3	ENST00000380456	-0.38405	0.0199
DGCR8	NM_022720	-0.37698	0.0199
SLC22A18	NM_183233	-0.3764	0.0195
LOC653080	AK097091	-0.37018	0.0198
C11orf75	NM_020179	-0.37	0.0199

REFERENCES

1. Pignon JP, Bourhis J, Domenge C *et al*. Chemotherapy added to locoregional treatment for head and neck squamous-cell carcinoma: three meta-analyses of updated individual data. MACH-NC Collaborative Group. Meta-Analysis of Chemotherapy on Head and Neck Cancer. Lancet 2000;355:949-955.
2. Akervall J, Guo X, Qian CN *et al*. Genetic and expression profiles of squamous cell carcinoma of the head and neck correlate with cisplatin sensitivity and resistance in cell lines and patients. Clin. Cancer Res. 2004;10:8204-8213.
3. Pramana J, van den Brekel MW, van Velthuysen ML *et al*. Gene Expression Profiling to Predict Outcome after Chemoradiation in Head and Neck Cancer. Int. J. Radiat. Oncol. Biol. Phys. 2007;69:1544-1552.
4. Bonnet D and Dick JE. Human acute myeloid leukemia is organized as a hierarchy that originates from a primitive hematopoietic cell. Nat. Med. 1997;3:730-737.
5. Al Hajj M, Wicha MS, Benito-Hernandez A *et al*. Prospective identification of tumorigenic breast cancer cells. Proc. Natl. Acad. Sci. U. S. A 2003;100:3983-3988.
6. Bao S, Wu Q, McLendon RE *et al*. Glioma stem cells promote radioresistance by preferential activation of the DNA damage response. Nature 2006;444:756-760.
7. Shiras A, Chettiar ST, Shepal V *et al*. Spontaneous transformation of human adult nontumorigenic stem cells to cancer stem cells is driven by genomic instability in a human model of glioblastoma. Stem Cells 2007;25:1478-1489.
8. Rosland GV, Svendsen A, Torsvik A *et al*. Long-term cultures of bone marrow-derived human mesenchymal stem cells frequently undergo spontaneous malignant transformation. Cancer Res. 2009;69:5331-5339.
9. Teng IW, Hou PC, Lee KD *et al*. Targeted Methylation of Two Tumor Suppressor Genes Is Sufficient to Transform Mesenchymal Stem Cells into Cancer Stem/Initiating Cells. Cancer Res. 2011;71:4653-4663.
10. Leemans CR, Braakhuis BJ, Brakenhoff RH. The molecular biology of head and neck cancer. Nat. Rev. Cancer 2011;11:9-22.
11. Aruffo A, Stamenkovic I, Melnick M *et al*. CD44 is the principal cell surface receptor for hyaluronate. Cell 1990;61:1303-1313.
12. Prince ME, Sivanandan R, Kaczorowski A *et al*. Identification of a subpopulation of cells with cancer stem cell properties in head and neck squamous cell carcinoma. Proc. Natl. Acad. Sci. U. S. A 2007;104:973-978.
13. Welters MJ, Fichtinger-Schepman AM, Baan RA *et al*. Relationship between the parameters cellular differentiation, doubling time and platinum accumulation and cisplatin sensitivity in a panel of head and neck cancer cell lines. Int. J. Cancer 1997;71:410-415.
14. Lin CJ, Grandis JR, Carey TE *et al*. Head and neck squamous cell carcinoma cell lines: established models and rationale for selection. Head Neck 2007;29:163-188.
15. Shevchenko A, Tomas H, Havlis J *et al*. In-gel digestion for mass spectrometric characterization of proteins and proteomes. Nat. Protoc. 2006;1:2856-2860.
16. Nesvizhskii AI, Keller A, Kolker E *et al*. A statistical model for identifying proteins by tandem mass spectrometry. Anal. Chem. 2003;75:4646-4658.
17. Quak JJ, Schrijvers HG, Brakkee JG *et al*. Expression and characterization of two differentiation antigens in human stratified squamous epithelia and carcinomas. Int. J. Cancer 1992;50:507-513.
18. Van Hal NL, van Dongen GA, Stigter-van Walsum M *et al*. Characterization of CD44v6 isoforms in head-and-neck squamous-cell carcinoma. Int. J. Cancer 1999;82:837-845.
19. Joshua B, Kaplan MJ, Doweck I *et al*. Frequency of cells expressing CD44, a head and neck cancer stem cell marker: correlation with tumor aggressiveness. Head Neck 2012;34:42-49.
20. Koukourakis MI, Giatromanolaki A, Tsakmaki V *et al*. Cancer stem cell phenotype relates to radio-chemotherapy outcome in locally advanced squamous cell head-neck cancer. Br. J. Cancer 2012;106:846-853.
21. Perez A, Neskey DM, Wen J *et al*. CD44 interacts with EGFR and promotes head and neck squamous cell carcinoma initiation and progression. Oral Oncol. 2012;49:306-313.
22. Pries R, Witrkopf N, Trenkle T *et al*. Potential stem cell marker CD44 is constitutively expressed in permanent cell lines of head and neck cancer. In Vivo 2008;22:89-92.

23. Wilson GD, Marples B, Galoforo S *et al*. Isolation and genomic characterization of stem cells in head and neck cancer. Head Neck 2012;35:1573-1582.
24. Esseghir S, Reis-Filho JS, Kennedy A *et al*. Identification of transmembrane proteins as potential prognostic markers and therapeutic targets in breast cancer by a screen for signal sequence encoding transcripts. J. Pathol. 2006;210:420-430.
25. Ichinoe M, Mikami T, Yoshida T *et al*. High expression of L-type amino-acid transporter 1 (LAT1) in gastric carcinomas: Comparison with non-cancerous lesions. Pathol. Int. 2011;61:281-289.
26. Imai H, Kaira K, Oriuchi N *et al*. L-type amino acid transporter 1 expression is a prognostic marker in patients with surgically resected stage I non-small cell lung cancer. Histopathology 2009;54:804-813.
27. Kaira K, Oriuchi N, Imai H *et al*. Prognostic significance of L-type amino acid transporter 1 expression in resectable stage I-III nonsmall cell lung cancer. Br. J. Cancer 2008;98:742-748.
28. Kaira K, Oriuchi N, Imai H *et al*. Prognostic significance of L-type amino acid transporter 1 (LAT1) and 4F2 heavy chain (CD98) expression in early stage squamous cell carcinoma of the lung. Cancer Sci. 2009;100:248-254.
29. Kaira K, Oriuchi N, Imai H *et al*. CD98 expression is associated with poor prognosis in resected non-small-cell lung cancer with lymph node metastases. Ann. Surg. Oncol. 2009;16:3473-3481.
30. Kaira K, Takahashi T, Abe M *et al*. CD98 expression is associated with the grade of malignancy in thymic epithelial tumors. Oncol. Rep. 2010;24:861-867.
31. Sakata T, Ferdous G, Tsuruta T *et al*. L-type amino-acid transporter 1 as a novel biomarker for high-grade malignancy in prostate cancer. Pathol. Int. 2009;59:7-18.
32. Shishido T, Uno S, Kamohara M *et al*. Transformation of BALB3T3 cells caused by over-expression of rat CD98 heavy chain (HC) requires its association with light chain: mis-sense mutation in a cysteine residue of CD98HC eliminates its transforming activity. Int. J. Cancer 2000;87:311-316.
33. Henderson NC, Collis EA, Mackinnon AC *et al*. CD98hc (SLC3A2) interaction with beta 1 integrins is required for transformation. J. Biol. Chem. 2004;279:54731-54741.
34. Feral CC, Nishiya N, Fenczik CA *et al*. CD98hc (SLC3A2) mediates integrin signaling. Proc. Natl. Acad. Sci. U. S. A 2005;102:355-360.
35. Armulik A, Velling TJohansson S. The integrin beta1 subunit transmembrane domain regulates phosphatidylinositol 3-kinase-dependent tyrosine phosphorylation of Crk-associated substrate. Mol. Biol. Cell 2004;15:2558-2567.
36. Verrey F. System L: heteromeric exchangers of large, neutral amino acids involved in directional transport. Pflugers Arch. 2003;445:529-533.
37. Gibbs S, Fijneman R, Wiegant J *et al*. Molecular characterization and evolution of the SPRR family of keratinocyte differentiation markers encoding small proline-rich proteins. Genomics 1993;16:630-637.